Temperature Dependence of Water Vibrational Spectrum: A Molecular Dynamics Simulation Study

Matej Praprotnik, Dušanka Janežič, and Janez Mavri*

National Institute of Chemistry, Hajdrihova 19, 1000 Ljubljana, Slovenia

Received: August 25, 2004; In Final Form: October 6, 2004

Vibrational spectroscopy studies show that the bulk water bending band becomes narrower with increasing temperature (Maréchal, Y. *J. Mol. Struct.* **1994**, *322*, 105). Since this counterintuitive effect is not associated with the quantum nature of nuclear motion a molecular dynamics (MD) simulation is expected to reproduce it even in the classical limit. We have performed a classical MD simulation of the flexible simple point charge (SPC) and extended SPC (SPC/E) water models to determine the temperature dependence of the bulk water vibrational spectrum. The intramolecular water potential proposed by Toukan and Rahman, including a stretch−bend coupling term, was applied. We performed MD simulations at −4 and 80 °C to compare the calculated vibrational spectra, in particular, the band associated with the bending mode, with the experiment. The experimentally determined narrowing of the bending band with increasing temperature is not reproducible by MD simulation with the applied force field. However, the results show that this approach successfully reproduces all other experimentally observed spectroscopic properties of bulk water.

1. Introduction

Water is a ubiquitous and exceptional liquid. For a comprehensive, recent attempt to collect all the known properties of water, including the effects of isotopic substitutions and spectroscopic properties, see ref 1.

Vibrational spectroscopy studies of bulk water in the range of 400−4000 cm^{-1} are rare.[2−5] A water molecule in the gas phase has three vibrational modes. Symmetric stretching appears at 3656 cm^{-1}, asymmetric stretching at 3755 cm^{-1}, and bending at 1594 cm^{-1}. In the liquid state, the infrared and Raman spectra become more complex due to vibrational overtones and intermolecular modes. The latter include librations associated with restricted rotations, hydrogen-bond stretchings, and modes involving coupled stretching and bending.[5] Both infrared and Raman spectra give evidence that there is a small but significant peak associated with coupling of the bending mode to the low-frequency libration modes. Temperature dependence of frequencies and intensities of various modes has been reported. In liquid water, the molecular stretching vibration frequencies are blue shifted upon raising the temperature, whereas the intramolecular bending vibrations frequencies are red shifted. The anomalous behavior has different interpretations.[3,6] The center of the combination modes can have different behavior with temperature, depending on the weight of each mode. As examples, the first overtone combination of symmetric and asymmetric stretch shows a shift from strongly hydrogen-bonded structures (6707 cm^{-1}) to weakly hydrogen-bonded structures (7082 cm^{-1}) with increasing temperature,[3] and the combination band at about 5200 cm^{-1} shifts to slightly higher wavenumbers with reduced hydrogen-bond strength.[6]

Recently, Maréchal thoroughly studied the temperature dependence of the vibrational spectrum of bulk water.[2] An important conclusion of his work was that the band associated with bending centered at about 1650 cm^{-1} becomes narrower with increasing temperature. Supercooled water at −4 °C has a broader band than water at 80 °C. This is a counterintuitive result since according to textbook statistical mechanics the molecular collisions should broaden the vibrational bending band with increasing temperature.[7] Since the same dependence was observed for deuterated forms of water, namely, for HDO and D_2O,[2] one can rule out the effects arising from the quantum nature of nuclear motion. Classical molecular dynamics (MD) simulation with a more or less complex potential is therefore the method of choice for a computational study of the liquid state.

Recently, numerous molecular simulations of water have been performed using various models.[8−17]

In this article, we performed a classical MD simulation with the flexible simple point charge (SPC) and flexible extended SPC (SPC/E) water models[18,19] to model the temperature dependence of the vibrational spectrum. The applied water models were based on the Toukan and Rahman potential,[20] which combines SPC nonbonding terms,[18] and an intramolecular part that includes the stretch−bend coupling term first introduced by Kuchitsu and Morino.[21] On top of that, the models applied in this work also include the reaction field treatment of long-range electrostatics.[22−24] The vibrational spectrum envelope was calculated by a Fourier transform of the velocity autocorrelation function. Our simulations were performed at two temperatures: at −4 °C, corresponding to supercooled water, and at 80 °C. The calculated vibrational spectra, in particular, the band associated with the bending mode, are compared with the experiment. The organization of this article is as follows. Section 2 describes the applied simulation methods. The results and discussion are summarized in section 3, followed by conclusions in section 4.

2. Computational Methods

2.1 Symplectic MD Integrator. We have employed in our simulations a recently derived split integration symplectic method (SISM),[25−27] a second-order symplectic MD integrator.

* Corresponding author. E-mail: janez@kihp2.ki.si.

10.1021/jp046158d CCC: $27.50
Published on Web 11/20/2004

In derivation of the SISM we split the Hamiltonian H of a system into two parts

$$H = H_0 + H_r \tag{1}$$

where H_0 is the part of the Hamiltonian, which can be solved analytically and H_r is the remaining part.

Then a second-order approximation for the classical propagator $\exp(\Delta t\hat{L}_H)$ known as the generalized leapfrog scheme[28,29]

$$\exp\left(\frac{\Delta t}{2}\hat{L}_{H_0}\right)\exp(\Delta t\hat{L}_{H_r})\exp\left(\frac{\Delta t}{2}\hat{L}_{H_0}\right) + \mathcal{O}(\Delta t^3) \tag{2}$$

defines the SISM if the propagation by $\exp(\Delta t/2\hat{L}_{H_0})$ is solved analytically using normal modes of an isolated molecule,[30−33] while the propagation by $\exp(\Delta t\hat{L}_{H_r})$ is solved numerically.

Owing to the analytical treatment of high-frequency molecular vibrations, the SISM is especially accurate and efficient for computing the vibrational spectrum. Since the vibrational spectrum is one of the most sensitive properties with respect to the simulation protocol, application of such an accurate integrator is justified.

2.2 Simulation Protocol. MD simulations were implemented for a system of 2048 flexible simple point charge (SPC) water molecules[18] with the intramolecular potential proposed by Toukan and Rahman[20] in a cubic box with periodic boundary conditions using the minimum image convention. The MD Hamiltonian was of the following form[20,34,35]

$$H = \sum_i \frac{\mathbf{p}_i^2}{2m_i} + \sum_k \sum_{l=1}^{2} D_e[1 - \exp(\alpha\Delta r_{l_k})]^2 + \frac{1}{2}\sum_k k_\theta \Delta r_{3_k}^2 + \sum_k k_{r\theta}\Delta r_{3_k}(\Delta r_{1_k} + \Delta r_{2_k}) + \sum_k k_{rr}\Delta r_{1_k}\Delta r_{2_k} + \sum_{i>j}\left(\frac{e_i e_j}{4\pi e_0 r_{ij}} + 4\epsilon_{ij}\left[\left(\frac{\sigma_{ij}}{r_{ij}}\right)^{12} - \left(\frac{\sigma_{ij}}{r_{ij}}\right)^{6}\right] + V_{RF}(r_{ij})\right) \tag{3}$$

where i and j run over all atoms and intramolecular interactions are excluded, k runs over all molecules, m_i is the mass of the ith atom, $\mathbf{p}_i$ is the linear momentum of the ith atom, Δr_{1_k}, Δr_{2_k} are the stretch in the O−H bond lengths, Δr_{3_k} is the stretch in the H−H distance of the kth molecule, D_e is the depth of the Morse potential, $a = (\sqrt{k_r}/2D_e)$, k_r, k_θ, $k_{r\theta}$, and k_{rr} are the force constants of intramolecular potential; e_i denotes the charge on the ith atom, ϵ_0 is the vacuum dielectric permittivity, r_{ij} is the distance between the ith and jth atoms, and ϵ_{ij} and σ_{ij} are the corresponding constants of the Lennard-Jones potential. The nonbonded interactions were calculated following the procedure described in refs 8, 23, and 24: the van der Waals and electrostatic interactions among all molecules inside the cutoff sphere of radius $R_c = 14$ Å were calculated explicitly while the long-range electrostatic interactions between molecules with the centers of mass at a distance beyond the cutoff radius R_c were included by the reaction field term[8,36,37]

$$V_{RF}(r_{ij}) = \frac{e_i e_j(\epsilon_{RF} - 1)r_{ij}^2}{4\pi\epsilon_0(2\epsilon_{RF} + 1)R_c^3} \tag{4}$$

The system outside the spherical cavity of radius R_c is thus treated as a dielectric continuum with a dielectric constant ϵ_{RF} corresponding to the experimental value at the given temperature, as listed in Table 3. We have chosen the reaction-field method to treat the long-range electrostatic interactions since it is known that the Ewald summation method[38] and related mesh methods impose an artificial periodicity in systems that are inherently nonperiodic, e.g., liquid water, and therefore can cause artifacts in molecular simulations.[39−44] The applied force field parameters are collected in Table 1.

TABLE 1: Parameters[a] of the Flexible SPC Model[18] of Water Molecule with Kuchitsu-Morino Intramolecular Potential[20,21]

parameter	value
r_0	1.0 Å
θ_0	109.47°
D_e	101.9188 kcal/mol
a	2.567 Å^{-1}
k_θ	328.645606 kcal/mol/Å^2
$k_{r\theta}$	−211.4672 kcal/mol/Å^2
k_{rr}	111.70765 kcal/mol/Å^2
e_H	$0.41e_0$
e_O	$-0.82e_0$
σ_{OO}	3.166 Å
ϵ_{OO}	0.1554 kcal/mol

[a] Parameter r_0 is the equilibrium O−H distance, θ_0 is the equilibrium value of angle H−O−H, and quantity e_0 is the positive unit charge. All force field parameters of the flexible SPC/E model[19] are the same except for the increased partial charges $e_H = 0.4238e_0$ and $e_O = -0.8476e_0$.

The first term in the Hamiltonian (3) is the kinetic energy of the system, the second term is the Morse potential defining the bond stretching potential, the third one describes the angle bending potential, the fourth and the fifth term are cross terms describing coupling between the internal coordinates, the sixth term is the Coulomb potential, the seventh term is the Lennard-Jones potential, and the last term is the reaction field term, respectively.

Although the original SPC water model is rigid and was originally designed to reproduce the experimental density and heat of evaporation of liquid water at 298 K, it is quite successful in reproducing most thermodynamic properties of water not only at ambient conditions but also in a wide range of state conditions, including the supercritical conditions.[45] As an improvement of the rigid model, the flexibility of the water molecule is incorporated by adding additional energy terms for stretching and bending to the potential function.[20,34,46,47] The flexible SPC water model can also account for corrections due to the self-polarization energy inherent in the potential as well as the correction to the average monomer energy when going from gas to liquid.[47] Also, the water spectroscopic properties are well reproduced including the experimentally observed solvent-induced red shift of the stretching band and the characteristic blue shift of the bending band upon going from gas to liquid.[20,34,47]

The flexible SPC water model[20] applied in this study is more realistic in reproducing the vibrational spectra than the flexible SPC water model developed in ref 47 or the flexible TIP3P (transferable intermolecular potential with three interaction sites) water model[48,49] since it uses the Morse function instead of the quadratic function for describing the bond stretching and includes an additional stretch−bend coupling term. As discussed in refs 20 and 46, this is the key factor to describe the experimentally observed red shift of the stretching band, which is due to both the liquid surrounding as well as the anharmonicity of the potential.

The chosen sizes of the cubic box were 39.5 and 39.9 Å corresponding to experimental densities of 1.0 and 0.972 g/cm^3 at −4 and 80 °C, respectively. The simulations were performed at two constant temperatures, −4 and 80 °C, using Berendsen's thermostat with the 0.1 ps coupling constants.[50]

The initial positions and velocities of the system atoms were chosen at random. Then the system was equilibrated for 100 ps to ensure that the velocities at a desired temperature assume a Maxwell distribution. Using the SISM with a 1.0 fs integration time step and these initial conditions two 500 ps MD simulations were performed and used for analysis. Performing MD simulations by the SISM with a 1.0 fs integration time step avoids all possible artifacts due to inaccurate integration.[27]

We have also performed two additional MD simulations at −4 and 80 °C with the same simulation protocol for a system of 2048 flexible extended SPC (SPC/E) water molecules.[19] In the SPC/E water model the self-polarization energy term is included in the effective pair potential. This is realized by the increased partial charges $e_H = 0.4238e_0$ on the hydrogen atoms and $e_O = -0.8476e_0$ on the oxygen atoms, where e_0 is the positive unit charge and all others force-field parameters are the same as the parameters of the flexible SPC model reported in Table 1.

2.3 Calculation of Vibrational Spectrum. The infrared (IR) absorption spectrum is obtained by Fourier transforming the dipole moment autocorrelation function as[51−53]

$$I(\omega) \propto \int_0^\infty \langle \boldsymbol{M}(t)\cdot\boldsymbol{M}(0)\rangle \cos(\omega t)\mathrm{d}t \tag{5}$$

where $I(\omega)$ is the spectral density, $\mathbf{M}(t)$ is the total dipole moment of the system at time t, and ω is the vibration frequency. $\mathbf{M}(t)$ is equal to the sum of all the individual dipole moments of the molecules in the simulation box

$$\mathbf{M}(t) = \sum_{i=1}^{m} \mu_i(t) \tag{6}$$

where $\mu_i(t)$ is the dipole moment of the ith molecule at time t and m is the number of molecules in the simulation box. The autocorrelation function of the dipole moment is given by[54,55]

$$\langle \mathbf{M}(t)\cdot\mathbf{M}(0)\rangle = \langle \sum_{j=1}^{n} e_j \mathbf{r}_j(t)\cdot \sum_{j=1}^{n} e_j \mathbf{r}_j(0)\rangle \tag{7}$$

where n is the number of all the atoms in the system, e_j is the fixed electric charge of the jth atom, and $\mathbf{r}_j(t)$ is the position vector of the jth atom at time t. The angular brackets represent an average taken over all time origins. The IR spectrum can be also computed using the dipole moment time derivative autocorrelation function[53−55]

$$\langle \sum_{j=1}^{n} e_j \mathbf{v}_j(t)\cdot \sum_{j=1}^{n} e_j \mathbf{v}_j(0)\rangle = \left\langle \sum_{j=1}^{n} e_j \frac{d\mathbf{r}_j(t)}{dt}\cdot \sum_{j=1}^{n} e_j \frac{d\mathbf{r}_j(0)}{dt}\right\rangle = \left\langle \frac{d\mathbf{M}(t)}{dt}\cdot\frac{d\mathbf{M}(0)}{dt}\right\rangle \tag{8}$$

The spectral density is then given as[54,55]

$$I(\omega) \propto \int_0^\infty \left\langle \frac{d\mathbf{M}(t)}{dt}\cdot\frac{d\mathbf{M}(0)}{dt}\right\rangle \cos(\omega t)dt = \int_0^\infty \langle \sum_{j=1}^{n} e_j \mathbf{v}_j(t)\cdot \sum_{j=1}^{n} e_j \mathbf{v}_j(0)\rangle \cos(\omega t)dt \tag{9}$$

The IR spectrum calculated by eq 9 differs from the IR spectrum using eq 5 only by its intensity.[54]

In strongly coupled molecular systems with a large number of atoms time autocorrelation functions (7) and (8) should decay to zero very rapidly within a small number of vibration periods.

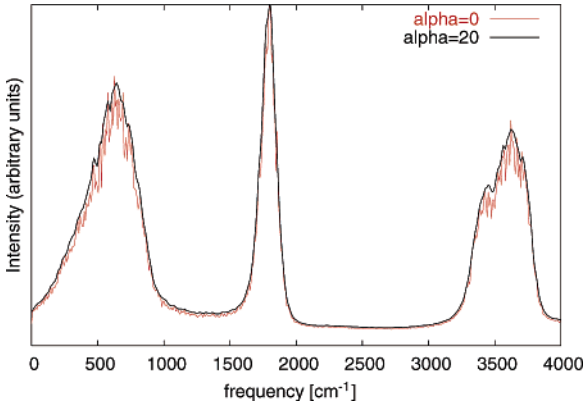

Figure 1. IR spectrum (arbitrary units) of water at $T = 80$ °C calculated by SISM for the flexible SPC water model with or without the application of the apodization function $\exp(-\alpha t^2)$ with $\alpha = 20$.

In MD simulations of systems with a relatively small number of atoms the obtained autocorrelation functions however fluctuate around the value of zero for much longer times. This artifact can be attributed to a small number of atoms and periodic boundary conditions. These fluctuations can be removed either by averaging together several individual correlation functions from statistically independent portions of the same trajectory or by applying an apodization function of a Gaussian type $\exp(-\alpha t^2)$ prior to the Fourier transform calculation.[54,56] The parameter α is chosen in a way that the amplitude of fluctuations asymptotically approach zero in the 0.5 ps time interval. The spectral density is then

$$I(\omega) \propto \int_0^\infty \langle \sum_{j=1}^{n} e_j \mathbf{v}_j(t)\cdot \sum_{j=1}^{n} e_j \mathbf{v}_j(0)\rangle \exp(-\alpha t^2)\cos(\omega t)dt \tag{10}$$

3. Results and Discussion

We determined the effect of using the apodization function $\exp(-\alpha t^2)$ in the calculation of a vibrational spectrum. In Figure 1 are presented the calculated vibrational spectra for the flexible SPC water model at $T = 80$ °C obtained by eqs 9 and 10, respectively, employing the fast Fourier transform (FFT) routine.[57] It can be observed that the spectrum computed by eq 10 is only smoothed with the respect to the corresponding spectrum obtained by using eq 9, while peak positions and line widths remain the same. Therefore, we have used eq 10 for all further evaluations of the vibrational spectra.

The calculated vibrational spectra of bulk water at $T = -4$ °C and $T = 80$ °C are depicted in Figure 2, which displays three characteristics frequency bands of bulk water corresponding to the stretching, bending, and librational motions of water molecules. Both the flexible SPC and SPC/E water models with the reaction field treatment of the long-range electrostatics were considered. Although the SPC/E model predicts improved self-diffusion and static dielectric constants and an improved liquid structure relative to the SPC model,[8] it is evident from Figures 2−5 that the results for the flexible SPC and SPC/E models are similar. The bending and libration bands of the flexible SPC/E water are positioned at slightly higher frequencies and the stretching band at a slightly lower frequency relative to the flexible SPC model. In both cases, the positions of the three characteristics frequency bands are in agreement with the experiment as indicated in Table 2 in which the experimental and calculated vibrational frequency are given for the gas and liquid phases of water. The solvent-induced red shift of the stretching band and the blue shift of the bending band upon

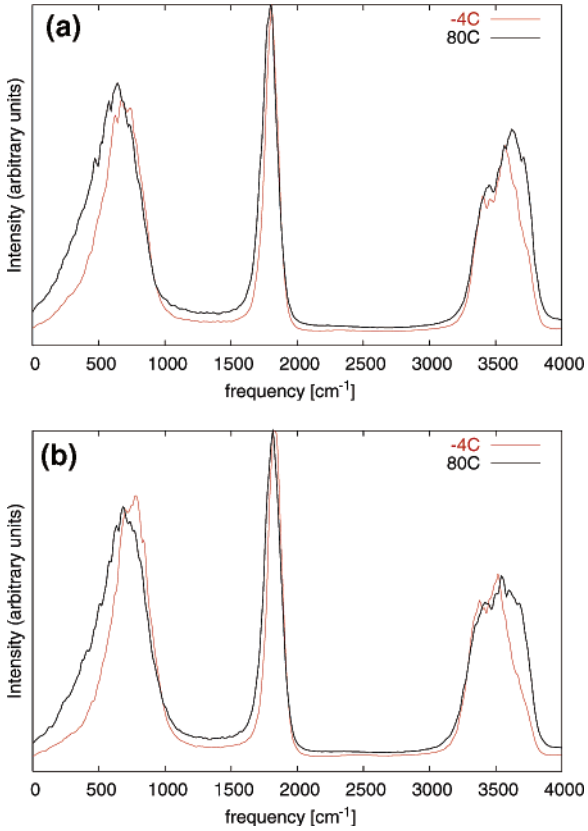

Figure 2. IR spectrum (arbitrary units) of water at $T = -4$ °C and $T = 80$ °C calculated by SISM (smoothed with $\alpha = 20$). (a) The flexible SPC water model. (b) The flexible SPC/E water model.

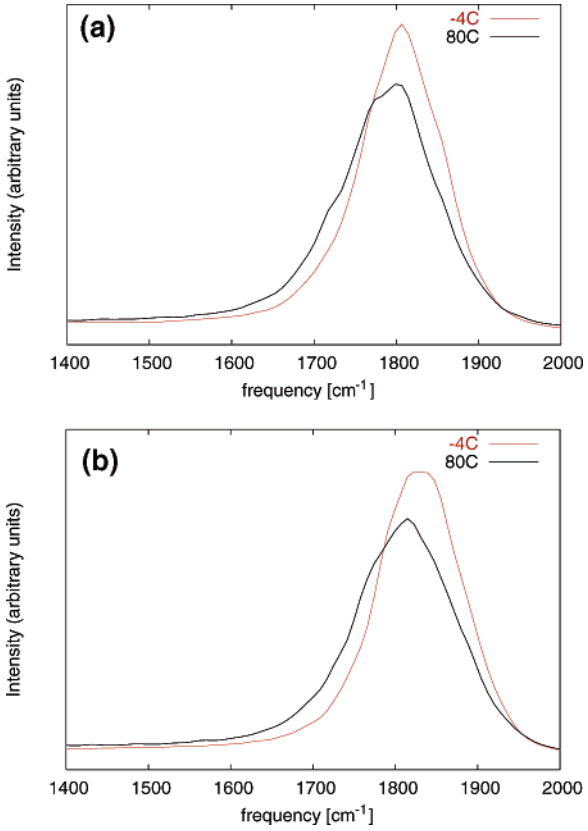

Figure 3. Bending peak (arbitrary units) of water at $T = -4$ °C and $T = 80$ °C calculated by SISM (smoothed with $\alpha = 20$). (a) The flexible SPC water model. (b) The flexible SPC/E water model.

TABLE 2: Experimental and Calculated Vibrational Frequencies of Water

	experiment[a]	calculated
gas phase	[cm^{-1}]	[cm^{-1}]
asymmetric stretch	3755	3965
symmetric stretch	3656	3836
bending	1594	1659
liquid phase (SPC)	[cm^{-1}]	[cm^{-1}]
stretching	3557	3564[b], 3621[c]
bending	1670	1806[b], 1790[c]
libration	597	675[b], 640[c]
liquid phase (SPC/E)	[cm^{-1}]	[cm^{-1}]
stretching	3557	3515[b], 3540[c]
bending	1670	1829[b], 1811[c]
libration	597	750[b], 685[c]

[a] Experimental values are taken from refs 46 and 58, where stretching and bending correspond to $T = 40$ °C and libration corresponds to supercooled water at $T = -15$ °C. [b] $T = -4$ °C. [c] $T = 80$ °C.

going from gas to liquid are well reproduced. Also, as can be observed from Figure 2, the blue shift of the stretching band as well as the red shifts of the bending and the librational band with an increasing temperature[2,47,58] are reproduced. This confirms that the quality of the applied water models is high enough to qualitatively reproduce spectroscopic properties of liquid water at given temperatures.

However, from Figure 3, which shows the corresponding bending bands at $T = -4$ °C and $T = 80$ °C, we can observe that the widths of both bands are approximately the same (≈60 cm^{-1}) in contrast to the experiment (≈40 cm^{-1} for $T = 80$ °C).[2]

Maréchal attributed the effect of narrowing of the bending band to the uniaxial rotational intermolecular motion. The explanation is based on the premise that the rotational motion around the symmetry axis is faster than rotation around the other two axes. Maréchal explains the effect by rotational energy levels that are above the classical potential barrier and therefore exhibit a diffusive character. This leads to rapid relaxation of bending vibrations and consequently to bending band narrowing with increasing temperature.[2]

Anisotropy of water rotational motion has been critically discussed by van der Spoel et al.[59] Experimental data give strong evidence that rotational motion is isotropic, while classical MD simulation using various effectively polarized water models gives significant anisotropy.[59] Therefore, MD simulation should reproduce the effect even in the classical limit.

Since, according to Kubo relations,[60] the bending band is expected to adopt a Lorentzian shape, we have fitted the obtained bending band at both temperatures by a Lorentzian curve of the form $f(x) = P/\pi\mu\{1 + [(x - \bar{x})/\mu]^2\}$. The results are presented in Figures 4 and 5 for $T = -4$ °C and $T = 80$ °C, respectively, for both water models. We have also fitted the computed bending bands by a fitting function of the Gaussian type and found that the agreement of the computed data with the Lorentzian curve is slightly better than the corresponding fit to the Gaussian curve (lower standard deviation (std) value[57]), which is in agreement with Kubo.[60] The parameter μ, which corresponds to the width of the Lorentzian curve, is slightly larger in the case of $T = 80$ °C. Therefore, we can conclude that our simulations did not reproduce the narrowing of the bending band with increasing temperature. The discrepancy between computed and experimental results could be attributed to the limitations of the water models employed.

To determine the possible effects of the system size and the simulation length, we also performed all simulations for a system of 256 molecules. The simulation protocol was the same as in

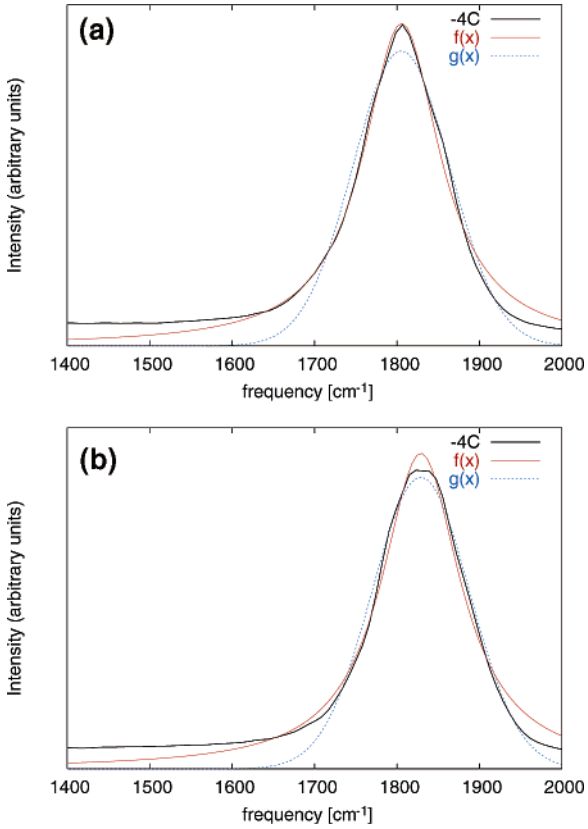

Figure 4. (a) Bending peak (arbitrary units) of water at $T = -4$ °C calculated by SISM using the flexible SPC water model (smoothed with $\alpha = 20$). Fitting function $f(x)$ is the Lorentzian curve defined as $f(x) = P/\pi\mu\{1 + [(x - \bar{x})/\mu]^2\}$ with $P = 0.85$, $\bar{x} = 1806$ cm^{-1}, and $\mu = 57$ cm^{-1} (std = 0.000159). Fitting function $g(x)$ is the Gaussian curve defined as $g(x) = a \exp[-(x - \bar{x})^2/2\sigma^2]$ with $a = 0.0043$, $\bar{x} = 1805$ cm^{-1}, and $\sigma = 59$ cm^{-1} (std = 0.000292). (b) The same as in (a) except for the flexible SPC/E water model. The fitting parameters are $P = 0.85$, $\bar{x} = 1829$ cm^{-1}, and $\mu = 58$ cm^{-1} (std = 0.000168) for the fitting function $f(x)$ and $a = 0.0043$, $\bar{x} = 1829$ cm^{-1}, and $\sigma = 59$ cm^{-1} (std = 0.000276) for the fitting function $g(x)$, respectively.

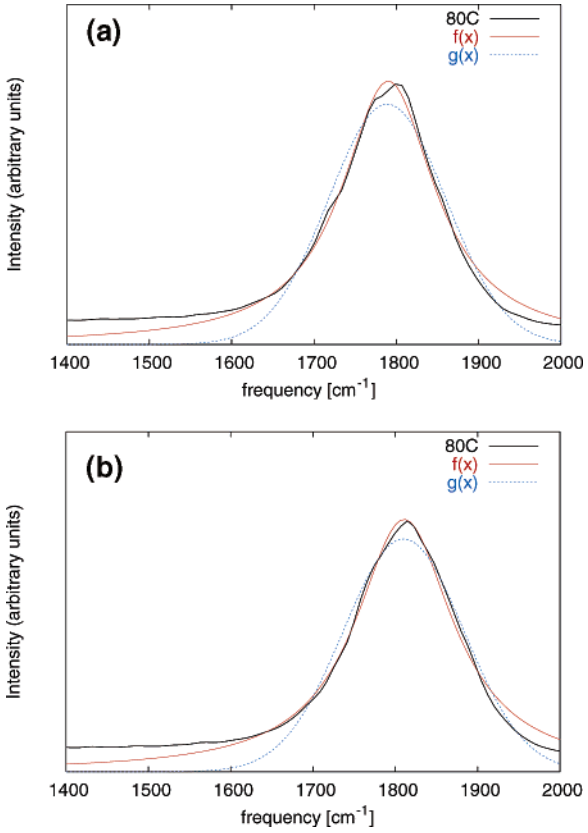

Figure 5. (a) Bending peak (arbitrary units) of water at $T = 80$ °C calculated by SISM using the flexible SPC water model (smoothed with $\alpha = 20$). Fitting function $f(x)$ is the Lorentzian curve defined as $f(x) = P/\pi\mu\{1 + [(x - \bar{x})/\mu]^2\}$ with $P = 0.84$, $\bar{x} = 1790$ cm^{-1}, and $\mu = 69$ cm^{-1} (std = 0.000143). Fitting function $g(x)$ is the Gaussian curve defined as $g(x) = a \exp[-(x - \bar{x})^2/2\sigma^2]$ with $a = 0.0035$, $\bar{x} = 1789$ cm^{-1}, and $\sigma = 71$ cm^{-1} (std = 0.000289). (b) The same as in (a) except for the flexible SPC/E water model. The fitting parameters are $P = 0.84$, $\bar{x} = 1811$ cm^{-1}, and $\mu = 72$ cm^{-1} (std = 0.000145) for the fitting function $f(x)$ and $a = 0.0034$, $\bar{x} = 1810$ cm^{-1}, and $\sigma = 73$ cm^{-1} (std = 0.000276) for the fitting function $g(x)$, respectively.

the example of 2048 molecules except for the cubic box sizes 19.75 and 19.95 Å, the cutoff radius $R_c = 9$ Å, and the 2 ns production run length. The computed spectra for the smaller (256 molecules) and larger (2048 molecules) system, shown in Figure 6 for the example of the system of the flexible SPC/E water molecules at $T = -4$ °C only, coincide regardless of the temperature and water model used. Therefore, we can conclude that the system size and effects due to periodic boundary conditions associated with it have no effect on the bending bandwidth.

To further validate our simulations and the models used, we also computed the static dielectric constant ϵ for the smaller system. The static dielectric constant ϵ is related to the fluctuations in the total dipole moment of the system as[22,61]

$$\epsilon = \frac{1 + [(\langle \mathbf{M}^2 \rangle - \langle \mathbf{M} \rangle^2)/3\epsilon_0 V k_B T][2\epsilon_{RF}/(2\epsilon_{RF} + 1)]}{1 - [(\langle \mathbf{M}^2 \rangle - \langle \mathbf{M} \rangle^2)/3\epsilon_0 V k_B T][1/(2\epsilon_{RF} + 1)]} \quad (11)$$

where $\mathbf{M}$ is the total dipole moment of the system, V is the total volume of the system, k_B is the Boltzmann constant, and T is the absolute temperature. The angular brackets denote a time average. The results for the flexible SPC and SPC/E water are listed in Table 3 together with the experimental values.[65] The computed values for both systems at both temperatures are

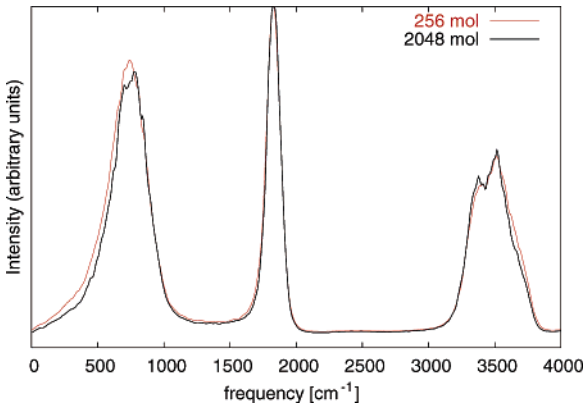

Figure 6. IR spectrum (arbitrary units) of water at $T = -4$ °C calculated by SISM for systems of 256 and 2048 flexible SPC/E water molecules.

slightly lower than the corresponding experimental values, but nevertheless higher than the reported literature values of the rigid SPC and SPC/E water models.[8,59,61] The better agreement of our results with the experiment is due to the flexibility of the flexible SPC and SPC/E models, which allow internal geometry changes and oscillation of the dipole moment of a water molecule.

Although these water models are unable to reproduce the experimentally observed bending band temperature narrowing,

TABLE 3: Experimental and Calculated Static Dielectric Constants of Liquid Water

	experiment[a]	SPC	SPC/E
T (°C)	ϵ	ϵ	ϵ
−4	87.7 (0 °C)	83.0	83.0
80	62.4 (75 °C)	55.7	58.4

[a] Experimental values are taken from refs 64 and 65.

they successfully reproduce overall spectroscopic properties of bulk water. We expect that the MD simulation using a more accurate potential function would also reproduce the experimentally observed bending band narrowing.

4. Conclusions

A classical MD simulation of the flexible SPC and SPC/E water models with the Kuchitsu-Morino intramolecular potential and the reaction field treatment of long-range electrostatics, together with an accurate symplectic SISM integrator, was used to study the temperature dependence of the water vibrational spectrum. All spectroscopic properties of liquid water, except the narrowing of the bending band at 1650 cm $^{-1}$, were reproduced.

To our belief, a quantum-dynamical treatment of nuclear motion would not improve the agreement between the calculated and experimental vibrational water spectrum, since experimental data indicates that even HDO and D_2O show the same effect.[2]

Speculations that the narrowing of the bending band of water at 80 °C could be caused by the molecules being more ordered than in supercooled water are ruled out by the neutron scattering studies showing no enhanced water ordering at 80 °C.[62] This means that the narrowing of the bending band is due to some other cause.

Perhaps we would be able to better describe this subtle effect by using less crude water models. However, within the class of nonpolarizable models the SPC/E model[19] combined with the reaction field gives the closest agreement with experimental data for various properties of bulk water.[59] Combined with the intramolecular potential proposed by Toukan and Rahman,[20] the SPC/E model should therefore be the preferred nonpolarizable water model for calculating the vibrational spectrum of bulk water.

The flexible SPC and SPC/E water models used in our study were developed from the rigid SPC and SPC/E water models by adding the intramolecular potential with no adjustment of the other model parameters.[20] In these models, it is therefore not considered that the internal vibrational motion will change the equilibrium configuration of a molecule.[35]

Further improvements of the water models could also be achieved by reparametrizing the parameters to be optimized for use with a reaction field[59,63] and by including an explicit polarization term in the model potential. Much work remains to be done in the development of this approach to explore its advantages and limitations. Besides the electronic polarizability, the electron transfer among the molecules might be important. A first principle simulation, such as Car-Parrinello molecular dynamics,[66] would be able to reproduce the temperature dependence of the vibrational spectrum of bulk water. With the ever increasing available computing power,[67] these simulations will become feasible.

Acknowledgment. The authors are grateful to Professors Yves Maréchal, Alenka Luzar, and Mauro Boero, and to Urban Borštnik for many stimulating discussions, and they also wish to thank the anonymous referees for their careful reading of the manuscript, their fruitful comments, and suggestions. This work was supported by the Ministry of Education, Science and Sports of Slovenia under Grant No. P1-0002.

Note Added after ASAP Publication. The date of publication for ref 2 (also cited in abstract) was corrected and panels a and b of Figure 4 were interchanged. This paper was published on the Web on 11/20/04. The corrected version was reposted on 11/23/04.

References and Notes

(1) http://www.lsbu.ac.uk/water and references therein.
(2) Maréchal, Y. *J. Mol. Struct.* **1994**, *322*, 105.
(3) Segtnan, V. H.; Sasic, S.; Isaksson, T.; Ozaki, Y. *Anal. Chem.* **2001**, *73*, 3153.
(4) Downing, H. D.; Williams, D. *J. Geophys. Res.* **1975**, *80*, 1656.
(5) Pinkley, L.; Sethna, P.; Williams, D. *J. Opt. Soc. Am.* **1977**, *67*, 494.
(6) Galinski, E. A.; Stein, M.; Amendt, B.; Kinder, M. *Comp. Biochem. Physiol.* **1997**, *117*, 357.
(7) McQuarrie, D. A. *Statistical Mechanics*; University Science Books: Sausalito, 2000.
(8) Glättli, A.; Daura, X.; van Gunsteren, W. F. *J. Comput. Chem.* **2003**, *24*, 1087.
(9) Mark, P.; Nilsson, L. *J. Comput. Chem.* **2002**, *23*, 1211.
(10) Luzar, A. *J. Chem. Phys.* **2000**, *113*, 10663.
(11) Mahoney, M. W.; Jorgensen, W. L. *J. Chem. Phys.* **2001**, *114*, 363.
(12) van Maaren, P. J.; van der Spoel, D. *J. Phys. Chem. B* **2001**, *105*, 2618.
(13) Hermansson, K.; Alfredsson, M. *J. Chem. Phys.* **1999**, *111*, 1993.
(14) Marti, J. *J. Chem. Phys.* **1999**, *110*, 6876.
(15) Hess, B.; Saint-Martin, H.; Berendsen, H. J. C. *J. Chem. Phys.* **2002**, *116*, 9602.
(16) Boero, M.; Terakura, K.; Ikeshoji, T.; Liew, C.; Parrinello, M. *J. Chem. Phys.* **2001**, *115*, 2219.
(17) Asbury, J. B.; Steinel, T.; Stromberg, C.; Corcelli, S. A.; Lawrence, C. P.; Skinner, J. L.; Fayer, M. D. *J. Phys. Chem. A.*
(18) Berendsen, H. J. C.; Postma, J. P. M.; van Gunsteren, W. F.; Hermans, J. In *Intermolecular Forces*; Pullman, B., Ed.; Reidel: Dordrecht, 1981; p 331.
(19) Berendsen, H. J. C.; Grigera, J. R.; Straatsma, T. P. *J. Phys. Chem.* **1987**, *91*, 6269.
(20) Toukan, K.; Rahman, A. *Phys. Rev. B* **1985**, *31*, 2643.
(21) Kuchitsu, K.; Morino, Y. *Bull. Chem. Soc. Jpn.* **1965**, *38*, 814.
(22) Neumann, M. *Mol. Phys.* **1983**, *50*, 841.
(23) Neumann, M. *J. Chem. Phys.* **1985**, *82*, 5663.
(24) Neumann, M. *J. Chem. Phys.* **1986**, *85*, 1567.
(25) Janežič, D.; Praprotnik, M. *Int. J. Quantum Chem.* **2001**, *84*, 2.
(26) Praprotnik, M.; Janežič, D. *Cell. Mol. Biol. Lett.* **2002**, *7*, 147.
(27) Janežič, D.; Praprotnik, M. *J. Chem. Inf. Comput. Sci.* **2003**, *43*, 1922.
(28) Strang, G. *SIAM J. Numer. Anal.* **1968**, *5*, 506.
(29) Grubmüller, H.; Heller, H.; Windemuth, A.; Schulten, K. *Mol. Simul.* **1991**, *6*, 121.
(30) Wilson, E. B.; Decius, J. C.; Cross, P. C. *Molecular Vibrations*; McGraw-Hill Book Company, Inc.: New York, 1955.
(31) Brooks, B. R.; Janežič, D.; Karplus, M. *J. Comput. Chem.* **1995**, *16*, 1522.
(32) Janežič, D.; Brooks, B. R. *J. Comput. Chem.* **1995**, *16*, 1543.
(33) Janežič, D.; Venable, R. M.; Brooks, B. R. *J. Comput. Chem.* **1995**, *16*, 1554.
(34) Marti, J.; Padro, J. A.; Guardia, E. *J. Mol. Liq.* **1994**, *62*, 17.
(35) Lawrence, C. P.; Skinner, J. L. *Chem. Phys. Lett.* **2003**, *372*, 842.
(36) Tironi, I. G.; Sperb, R.; Smith, P. E.; van Gunsteren, W. F. *J. Chem. Phys.* **1995**, *102*, 5451.
(37) Tironi, I. G.; Luty, B. A.; van Gunsteren, W. F. *J. Chem. Phys.* **1997**, *106*, 6068.
(38) Ewald, P. *Ann. Phys.* **1921**, *64*, 253.
(39) Luty, B. A.; van Gunsteren, W. F. *J. Phys. Chem.* **1996**, *100*, 2581.
(40) Hünenberger, P.; McCammon, J. A. *J. Chem. Phys.* **1999**, *110*, 1856.
(41) Hünenberger, P.; McCammon, J. A. *Biophys. Chem.* **1999**, *78*, 69.
(42) Weber, W.; Hünenberger, P.; McCammon, J. A. *J. Phys. Chem. B* **2000**, *104*, 3668.
(43) Nymand, T. M.; Linse, P. *J. Chem. Phys.* **2000**, *112*, 6386.
(44) Walser, R.; Hünenberger, P.; van Gunsteren, W. F. *Proteins* **2001**, *44*, 509.
(45) Chialvo, A. A.; Cummings, P. T. *J. Chem. Phys.* **1996**, *105*, 8274.
(46) Dang, L. X.; Pettit, B. M. *J. Phys. Chem.* **1987**, *91*, 3349.

(47) Ferguson, D. M. *J. Comput. Chem.* **1995**, *16*, 501.
(48) Jorgensen, W. L.; Chandrasekhar, J.; Madura, J. D.; Impey, R. W.; Klein, M. L. *J. Chem. Phys.* **1983**, *79*, 926.
(49) Steinbach, P. J.; Brooks, B. R. *J. Comput. Chem.* **1994**, *15*, 667.
(50) Berendsen, H.; Postma, J.; van Gunsteren, W. F.; Nola, A. D.; Haak, J. *J. Chem. Phys.* **1984**, *81*, 3684.
(51) Guillot, B. *J. Chem. Phys.* **1991**, *95*, 1543.
(52) Leach, A. R. *Molecular Modelling*; Pearson Education Limited: Harlow, 2nd ed., 2001.
(53) Marti, J.; Padro, J. A.; Guardia, E. *Mol. Simul.* **1993**, *11*, 321.
(54) Boulard, B.; Kieffer, J.; Phifer, C. C.; Angell, C. A. *J. Non-Cryst. Solids* **1992**, *140*, 350.
(55) Bornhauser, P.; Bougeard, D. *J. Phys. Chem. B* **2001**, *105*, 36.
(56) Wilson, M.; Madden, P. A. *Phys. Rev. Lett.* **1996**, *77*, 4023.
(57) Press: W. H.; Flannery, B. P.; Teukolsky, S. A.; Vetterling, W. T. *Numerical Recipes: The Art of Scientific Computing*; Cambridge University Press: Cambridge, 1987.
(58) Chen, S. H.; Toukan, K.; Loong, C. K.; Price, D. L.; Teixeira, J. *Phys. Rev. Lett.* **1984**, *53*, 1360.
(59) van der Spoel, D.; van Maaren, P. J.; Berendsen, H. J. C. *J. Chem. Phys.* **1998**, *108*, 10220.
(60) Kubo, R. *Fluctuation, Relaxation, and Resonance in Magnetic Systems*; Oliver and Boyd: London, 1962.
(61) Smith, P. E.; van Gunsteren, W. F. *J. Chem. Phys.* **1994**, *100*, 3169.
(62) Luzar, A., private communication.
(63) Smith, P. E.; van Gunsteren, W. F. *Mol. Simul.* **1995**, *15*, 233.
(64) Weast, R. C., Ed. *CRC Handbook of Chemistry and Physics*, 66th ed.; CRC Press Inc.: Cleveland, 1986.
(65) Malberg, C. G.; Maryott, A. A. *J. Res. Nat. Bur. Stand.* **1956**, *56*, 1.
(66) Car, R.; Parrinello, M. *Phys. Rev. Lett.* **1985**, *55*, 2471.
(67) Borštnik, U.; Hodošček, M.; Janežič, D. *J. Chem. Info. Comput. Sci.* **2004**, *44*, 359.